ELSEVIER

International Journal of Pharmaceutics 248 (2002) 239–246

international journal of pharmaceutics

www.elsevier.com/locate/ijpharm

A kinetic study of the chemical stability of the antimetastatic ruthenium complex NAMI-A

Marjan Bouma [a,*], Bastiaan Nuijen [a], Martine T. Jansen [a], Gianni Sava [b], Antonella Flaibani [c,1], Auke Bult [d], Jos H. Beijnen [a,d]

[a] *Department of Pharmacy and Pharmacology, Slotervaart Hospital, The Netherlands Cancer Institute, Louwesweg 6, 1066 EC Amsterdam, The Netherlands*

[b] *Fondazione Callerio, 34127 Trieste, Italy*

[c] *SIGEA Srl, 34012 Trieste, Italy*

[d] *Faculty of Pharmaceutical Sciences, Utrecht University, 3584 CA Utrecht, The Netherlands*

Received 7 May 2002; received in revised form 13 August 2002; accepted 13 August 2002

Abstract

NAMI-A is a novel ruthenium complex with selective activity against cancer metastases currently in Phase I clinical trials in The Netherlands. The chemical stability of this new agent was investigated utilizing a stability-indicating reversed-phase high performance liquid chromatographic assay with ultraviolet detection and ultraviolet/visible light spectrophotometry. The degradation kinetics of NAMI-A were studied as a function of pH, buffer composition, and temperature. Degradation of NAMI-A follows first-order kinetics at pH < 6 and zero-order kinetics at pH ≥ 6. A pH-rate profile, employing rate constants extrapolated to zero buffer concentration, was constructed, demonstrating that NAMI-A is most stable in pH region 3–4. The degradation rate is not significantly affected by specific buffer components. Storage temperature strongly influences the degradation rate.

Keywords: NAMI-A; Chemical stability; High performance liquid chromatography (HPLC)

1. Introduction

NAMI-A (imidazolium *trans*-tetrachloro(dimethylsulfoxide)imidazoleruthenium(III), H_2im[*trans*-$RuCl_4$(DMSO)Him], Fig. 1) is a novel ruthenium anticancer agent. Preclinical pharmacological studies with NAMI-A showed selective activity against lung metastases of murine tumors (Sava et al., 1998, 1999a,b,c) and a relatively low toxicity in mice and dogs (Bergamo et al., 2000; Cocchietto and Sava, 2000; Sava and Cocchietto, 2000). Its action seems to be independent of the origin (type of primary tumor) and stage of growth of the metastases (Bergamo et al., 1999; Sava et al., 1999b,c). NAMI-A possesses no appreciable in vitro tumor cell cytotoxicity (Bergamo et al., 1999,

* Corresponding author. Tel.: +31-20-512-4733; fax: +31-20-512-4753

E-mail address: apmbo@slz.nl (M. Bouma).

[1] Present address: Eurand International S.p.A., Trieste, Italy.

0378-5173/02/$ - see front matter
PII: S0378-5173(02)00460-X

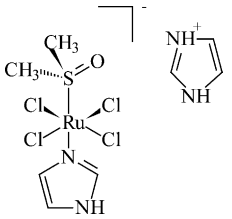

Fig. 1. Chemical structure of NAMI-A, molecular weight = 458.18 g/mol, molecular formula: $C_8H_{15}Cl_4N_4ORu(III)S$.

2000; Sava et al., 1999a; Zorzet et al., 2000), although an interaction with cell cycle regulation has been observed in a transient accumulation of cells in the G_2/M phase (Bergamo et al., 1999, 2000; Sava et al., 2000; Zorzet et al., 2000). Furthermore, NAMI-A increases the capsule thickness around the primary tumor and the extracellular matrix around tumor blood vessels, thereby preventing tumor cells from invading surrounding tissue and blood vessels (Sava et al., 1998; Zorzet et al., 2000). More recently, NAMI-A was shown to inhibit matrix metalloproteinases and to induce antiangiogenic effects (Vacca et al., 2002).

Based on its promising activity and toxicity profile, NAMI-A is developed as a potential anticancer agent and has currently entered Phase I clinical trials. Before a suitable pharmaceutical formulation can be developed for a new drug substance, it is important to gain insight into the stability of the agent in different types of solutions. This study was initiated with the objective to obtain detailed knowledge on the degradation kinetics of NAMI-A in aqueous solution, including the effects of several parameters such as pH, buffer composition, and temperature on the degradation process.

2. Materials and methods

2.1. Chemicals

NAMI-A was supplied by SIGEA Srl (Trieste, Italy). Methanol (HPLC grade) was obtained from Biosolve Ltd. (Amsterdam, The Netherlands) and distilled water from B. Braun Medical (Melsungen, Germany). Trifluoromethanesulfonic acid, sodium acetate trihydrate, acetic acid 96% (v/v), sodium dihydrogen phosphate dihydrate, disodium tetraborate decahydrate, sodium carbonate (anhydrous), sodium citrate monohydrate, hydrochloric acid 37%, sodium chloride, perchloric acid (70–72% (w/v)) and sodium hydroxide pellets were purchased from Merck (Darmstadt, Germany). Sodium dodecylsulphate was obtained from Fluka Chimica GmbH (Buch, Switzerland). All reagents were of analytical grade and used without further purification.

2.2. Buffer solutions

For the kinetic studies the following aqueous buffer solutions were used: pH 1–5, acetate; pH 6–11, phosphate. Buffers were prepared in concentrations of 0.01, 0.10 and 1.0 M. The pH values were measured using a Model 654 pH meter (Metrohm AG, Herisau, Switzerland).

2.3. Kinetic experiments

2.3.1. Influence of pH and buffer strength

The degradation reactions were initiated by adding 240 μl of a freshly prepared 50 mg/ml stock solution of NAMI-A in distilled water to 11.76 ml buffer solution, resulting in test solutions with a NAMI-A concentration of 1.0 mg/ml. The solutions were stored in glass test tubes, protected from light. All kinetic studies were conducted at 20–23 °C, unless otherwise stated. At appropriate time intervals, 500 μl samples were withdrawn from the test solutions, diluted 1:1 with mobile phase in an autosampler vial, and injected into the stability-indicating HPLC system for analysis. Furthermore, at selected time points, samples were analyzed by UV/VIS spectrophotometry. For all solutions, the pH in time was measured and adjusted as necessary to keep it constant. All kinetic experiments were performed in duplicate.

2.3.2. Influence of temperature

The effect of temperature on the degradation of NAMI-A was studied at pH 3 (0.1 M acetate buffer) and pH 7 (0.1 M phosphate buffer) in the temperature range of 4–37 °C. The test solutions were prepared as described above, with the use of

pre-warmed or cooled buffer solutions. The temperatures of the test solutions were kept constant in a thermostatically controlled water bath or refrigerator.

2.4. High performance liquid chromatography (HPLC)

The HPLC system consisted of a model SP8800 ternary pump (Thermo Separation Products (TSP), Fremont, CA, USA), a model 996 photo diode array (PDA) detector (Waters, Milford, MA, USA) and a model SP8880 autosampler (TSP). Chromatograms were processed using MILLENIUM® software (Waters). Separation was achieved using a μBondapak C18 column (Waters), protected with a C8 guard column (Security Guard, Phenomenex, Torrance, CA, USA). The mobile phase consisted of 0.50 mM sodium dodecylsulphate in 3% methanol, acidified to pH 2.5 using trifluoromethanesulfonic acid (triflic acid). The flow rate was 0.5 ml/min and the system was operated at ambient temperature. The detection wavelength was 358 nm and on-line spectral analysis was carried out with the PDA system. The injection volume was 20 μl. A run time of 10 min was employed for both the standard samples (calibration curve and quality control) and of 30 min for the samples under investigation. Employing this HPLC system, NAMI-A produces a peak with a retention time of approximately 4.1 min.

Calibration curves of standard NAMI-A solutions in distilled water were linear ($r > 0.98$) in the concentration range of interest (1–600 μg/ml).

2.5. Ultraviolet/visible light (UV/Vis) spectrophotometry

UV/Vis spectra were recorded with a Model UV/VIS 918 spectrophotometer (GBC Scientific Equipment, Victoria, Australia) equipped with a DELL personal computer and an Epson LX-400 printer. Spectra were recorded from 800 to 225 nm. Samples of the test solutions were diluted with distilled water to a theoretical concentration of 100 μg/ml before measurement.

2.6. Calculations

2.6.1. Order of reaction

The order of reaction was calculated using the graphic method as described by A. Martin (Martin, 1993). Zero, first and second order graphs were drawn for each pH and each buffer concentration by plotting time versus NAMI-A concentration, ln NAMI-A concentration, and 1/(NAMI-A concentration), respectively. The correlation coefficient of each graph was calculated, and the plot with the best linearity described the order of the reaction in the best manner. The observed rate constant (k_{obs}) was the slope (multiplied by -1) of the best-fitting graph. Half-times were determined by entering the appropriate values into the Eqs. (1) and (2) for zero and first order reactions, respectively:

$$t_{1/2} = \frac{a}{(2 \times k_{obs})} \quad (1)$$

$$t_{1/2} = \frac{\ln 2}{k_{obs}} \quad (2)$$

where a is the initial NAMI-A concentration (M).

3. Results and discussion

3.1. Degradation of NAMI-A

3.1.1. Degradation pathway and general observations

NAMI-A (Fig. 1) consists of a ruthenium atom with six ligands: four chloride ions, one DMSO group and one imidazole group. All of these ligands can be replaced by water molecules, hydroxide ions, or buffer components, resulting in a wide range of possible degradation products. A degradation pathway as depicted in Fig. 2 has been proposed for NAMI-A (Mestroni et al., 1994; Sava et al., 1999a). The structural elucidation of the various degradation products was based on UV/Vis spectrophotometry and NMR spectroscopy. NMR spectroscopy showed that neither DMSO nor the imidazole ligand are readily replaced in aqueous solution (Mestroni et al.,

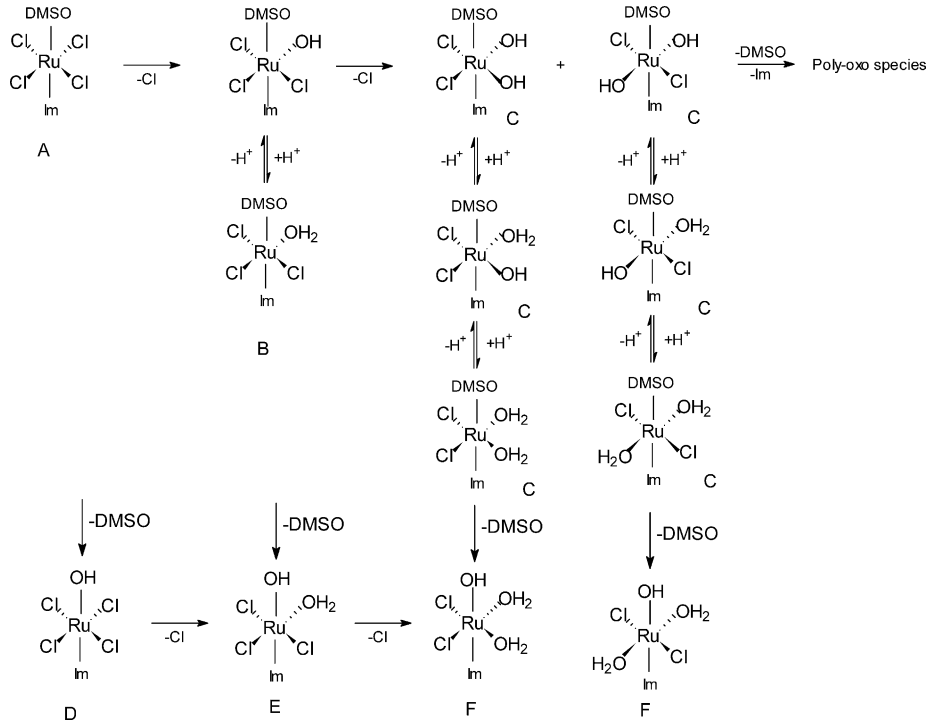

Fig. 2. Proposed degradation mechanism of NAMI-A (Mestroni et al., 1994; Sava et al., 1999a).

1994; Sava et al., 1999a), except in acidic solutions, where the DMSO group is hydrolyzed as well as the chloride ligands (Bouma et al., 2002; Sava et al., 2002). The degradation of NAMI-A thus consists of stepwise hydrolysis of the chloride ligands, in acidic media accompanied by hydrolysis of the DMSO group, followed by formation of poly-oxo species. This last step can be visually observed by darkening of the solutions.

Upon degradation in aqueous buffer solutions, when stored protected from light, the UV/Vis spectrum of NAMI-A changes as depicted in Fig. 3. Initially, two isosbestic points are present, at 274 and 358 nm, suggesting a single transformation in the chromophore in the early stages of degradation (substitution of ligands), the duration of which is dependent on the pH of the buffer solution. Thereafter, the spectrum began to distort the isosbestic points, providing evidence of secondary degradation, which could be caused by further substitution of ligands, polymerization, or oxidation or reduction of the chromophore Ru(III). The same changes were observed in all buffered

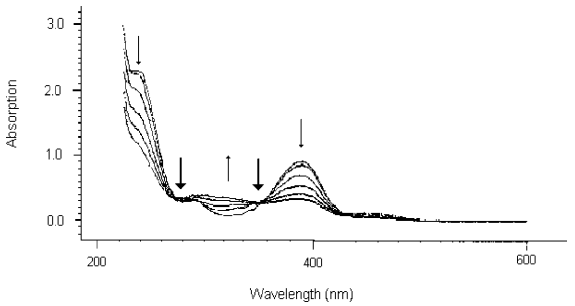

Fig. 3. Change in UV/Vis spectrum of a solution of 100 μg/ml NAMI-A in distilled water in time from $t = 0$ to 96 h (stored at 20–25 °C in the dark). The directions of the small arrows indicate an increase or decrease of absorption upon degradation; the large arrows indicate the isosbestic points at 274 and 358 nm.

NAMI-A solutions, although different time spans were required for these changes in the UV/Vis spectrum.

If unadjusted in time, the pH of all NAMI-A solutions changed to approximately 3.5 (as depicted in Fig. 4 for a solution of NAMI-A in water), indicating the formation of products with

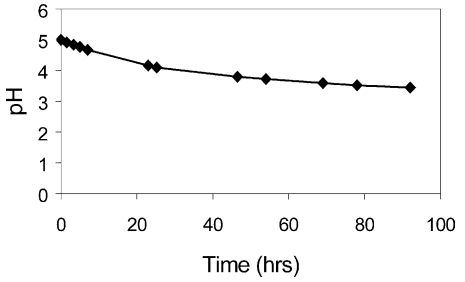

Fig. 4. Decrease in pH of a 1 mg/ml solution of NAMI-A in distilled water with time.

acidic properties ($pK_a \sim 3.5$) and/or protons. As depicted in Fig. 2, hydrolysis of NAMI-A and subsequent establishment of a equilibrium between the aqua and hydroxy products is accompanied by formation of protons, and thus lowering of the pH. The kinetic studies were thus performed in buffers. However, even the buffer solutions, especially those of alkaline pH and low molarity, needed occasional addition of base or acid to keep the pH constant.

Color changes were observed during the course of degradation. Whereas the color of all solutions immediately after preparation was yellow and all UV/VIS spectra at that time were identical, the solutions at acidic and neutral pH all darkened and in time turned brown, although the time it took for the color change varied (pH 1:96 h, pH 7:4 h). The solutions at pH 8–11 turned a lighter yellow color, although these solutions were examined for a maximum of 40 min. Color changes indicate a change in chromophore. Darkening of the solution has been ascribed to formation of poly-oxo or hydroxy species, while loss of color of NAMI-A solutions has been described for reduction of the ruthenium atom from Ru(III) to Ru(II) (Mestroni et al., 1994; Sava et al., 1999a, 2002).

3.2. Degradation kinetics

3.2.1. Analytical procedures and influence of pH

Degradation of NAMI-A can be followed using the presented HPLC method, which was proven to be stability-indicating, precise and accurate (Bouma et al., 2002). Fig. 5A and B show typical HPLC chromatograms of a decomposition mixture of NAMI-A at about one half-life in acidic and neutral media, respectively. Degradation products appear as separate peaks and no degradation products co-elute with the NAMI-A peak. In the neutral and alkaline reaction mixtures tailing of the NAMI-A peak was observed, as can be observed in Fig. 5B. UV/Vis analysis of the complete peak, including the tailing portion, showed the presence of only NAMI-A. Furthermore, no increase of the tailing area was observed in time, as would be expected for overlapping peaks in which one peak was a degradation product. It appeared that one or more of the components present in the neutral and alkaline buffers caused an interaction between NAMI-A and the column material, but not between the degradation products and the column material.

However, upon injection of the solutions to which sodium chloride had been added, the HPLC chromatograms showed two non-separated peaks covering the retention time (t_R) range of 3.7–5.3 min. Both peaks contained NAMI-A, as was determined from their UV/Vis spectra, but quantification became impossible by the formation of these two peaks. This effect prohibited the investigation of the influence of the ionic strength (μ) on the degradation of NAMI-A. These investigations require addition of various amounts of salts such as sodium chloride to the buffer solutions. Thus, the separation between NAMI-A and its degradation products in the HPLC chromatograms justifies use of the HPLC method for this kinetic study, but not in sodium chloride-containing solutions.

The peak attributed to the mono-hydroxy or aqua species (compound B in Fig. 2) (Bouma et al., 2002), with a t_R at 6.9 min, relative t_R 1.7, and maxima in its UV/Vis spectrum at 360 and 420 nm, is formed in all solutions. It is the only degradation product initially formed at pH values ≥ 6 and its formation is pH-dependent. At higher pH values, the rate and extent to which it is formed increases. At pH values < 6, more degradation products are formed. The degradation product at t_R 5.8 min (relative t_R 1.4, maxima in its UV/Vis spectrum at 326 and 374 nm) is only formed in solutions at pH < 6 and has not yet been positively identified, but could be any of the DMSO-free products depicted in Fig. 2 (Bouma et al., 2002). Its formation is also pH-dependent, with higher

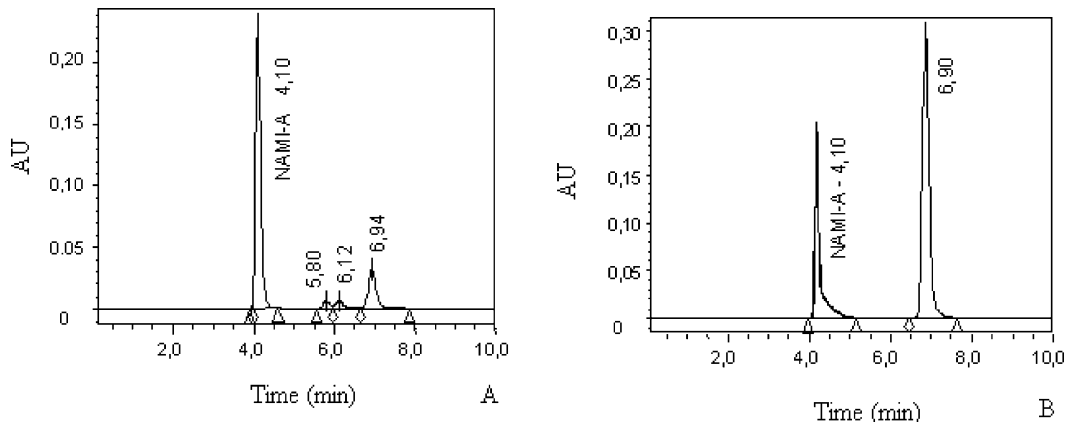

Fig. 5. (A) HPLC chromatogram of partly degraded NAMI-A in 0.1 M acetate solution at pH 4 after 48 h; (B) HPLC chromatogram of partly degraded NAMI-A in 0.1 M phosphate solution at pH 7 after 1.75 h.

amounts at lower pH values. The degradation product at t_R 6.1 min (relative t_R 1.5, maxima in its UV/Vis spectrum at 367 and 430 nm) is only formed at pH values <4, appears to a larger extent in more acidic solutions, and has not yet been identified.

3.2.2. Order of reaction

The degradation of NAMI-A in solutions at pH 1–5 follows (pseudo) first-order kinetics. This is indicated by the linearity of the plots ($r^2 > 0.99$) of time versus natural logarithm of residual NAMI-A concentration. At pH ≥ 6, however, degradation follows zero-order kinetics (r^2 for the time vs. concentration plots: 0.91–0.99).

The degradation products with a relative t_R of 1.4 and 1.5 were only formed at pH <6 and <4, respectively, and were not present in solutions of higher pH. Furthermore, color changes in acidic solutions differed from those in alkaline conditions. The observed changes indicated a difference in the main NAMI-A degradation mechanism in solutions at pH 1–5 and ≥ 6, which is in agreement with the calculated difference in order of reaction. Table 1 lists observed rate constants and half-lives of the different buffer solutions.

The order determinations could only be performed for the solutions with a pH ≤ 10. The solution at pH 11 (and higher) showed immediate and complete degradation upon dissolution of NAMI-A and could therefore not be included.

3.2.3. Influence of pH

Since the degradation of NAMI-A is strongly pH-dependent, it is important to keep the pH constant during the experiments. The kinetic experiments were therefore performed in buffer solutions. The overall observed rate constant for the degradation of NAMI-A in buffer solutions of pH 1–5 (following (pseudo) first-order kinetics) is:

$$k_{obs} = k_0 + k_H[H^+] + k_{OH}[OH^-] + k_{buffer}[buffer] \quad (3)$$

where k_0 is the (pseudo) first-order rate constant for degradation in water only, and k_H and k_{OH} are the second order rate constants for proton and hydroxyl-catalyzed degradation, respectively. The term $k_{buffer}[buffer]$ represents the sum of the second-order rate constants for the degradation catalyzed by each of the buffer components multiplied by its concentration. To obtain the specific rate constant (k') at each pH, incorporating only proton (H^+), hydroxide (OH^-) and water (H_2O) catalysis, the observed rate constants (k_{obs}) were corrected for buffer influence by plotting the k_{obs} against buffer concentration and extrapolating to zero buffer concentration. A linear relationship existed at each pH (for all pH values) between k_{obs} and the buffer concentration. The obtained k' is defined by Eq. (4):

$$k' = k_0 + k_H[H^+] + k_{OH}[OH^-] \quad (4)$$

The calculated values for k' were used in the

Table 1
Influence of buffer concentration on k_{obs} and $t_{1/2}$ of the degradation of NAMI-A

pH	[Buffer] (M)	k_{obs} (per s)	$t_{1/2}$ (h)*	pH	[Buffer] (M)	k_{obs} (M per s)	$t_{1/2}$ (h)*
1	0.01	5.41×10^{-6}	35.5	6	0.01	2.77×10^{-8}	11.1
	0.1	5.50×10^{-6}	35.0		0.1	2.78×10^{-8}	11.1
	1	5.56×10^{-6}	34.7		1	5.55×10^{-8}	4.7
2	0.01	5.56×10^{-6}	34.7	7	0.01	1.39×10^{-7}	2.3
	0.1	5.08×10^{-6}	37.9		0.1	1.94×10^{-7}	1.5
	1	5.44×10^{-6}	35.4		1	1.67×10^{-7}	1.5
3	0.01	3.39×10^{-6}	56.8	8	0.01	10.6×10^{-7}	0.3
	0.1	3.94×10^{-6}	48.8		0.1	8.61×10^{-7}	0.3
	1	6.19×10^{-6}	31.1		1	6.94×10^{-7}	0.3
4	0.01	3.11×10^{-6}	61.9	9	0.01	1.64×10^{-6}	0.2
	0.1	3.88×10^{-6}	49.5		0.1	1.69×10^{-6}	0.1
	1	5.31×10^{-6}	36.3		1	2.58×10^{-6}	0.1
5	0.01	2.88×10^{-6}	66.6	10	0.01	30.8×10^{-7}	0.1
	0.1	6.72×10^{-6}	28.6		0.1	9.44×10^{-7}	0.3
	1	14.4×10^{-6}	13.3		–	–	–

construction of the pH-rate profile (Fig. 6). As the units for k′ were different for the first and zero-order reactions (pH 1–5 and 6–10, respectively), two separate pH-rate profiles were constructed for the different types of reaction. Between pH 5 and 6, a combination of first and zero-order kinetics may prevail. A solution at pH 3.5 provides maximal stability for NAMI-A. Neither of the profiles shows a slope of ± 1, indicating that at $2 < \text{pH} < 3$ a combination of solvent and proton catalysis takes place and at $\text{pH} > 4$, a combination of solvent and hydroxyl catalysis. It was shown previously that the rate of the first hydrolytic step during degradation of NAMI-A, leading to formation of the mono-aqua or hydroxy species (compound B in Fig. 2), is catalyzed by Ru(II) species (Mestroni et al., 1994; Sava et al., 1999a, 2002). Thus, beside general acid–base and solvent catalysis, catalysis such as caused by Ru(II) species, formed by reduction of NAMI-A, additionally could take place.

3.2.4. Influence of buffers

Table 1 shows the influence of buffer concentration on the rate of degradation of NAMI-A. In general, NAMI-A degradation rates increase with increasing buffer concentration, which points to an interaction of NAMI-A with the buffer components.

To examine whether the type of buffer influenced the rate of degradation, 0.1 M carbonate and borate buffers at pH 9, and 0.1M citrate buffer and hydrochloric acid at pH 3 were prepared and degradation in these buffers was

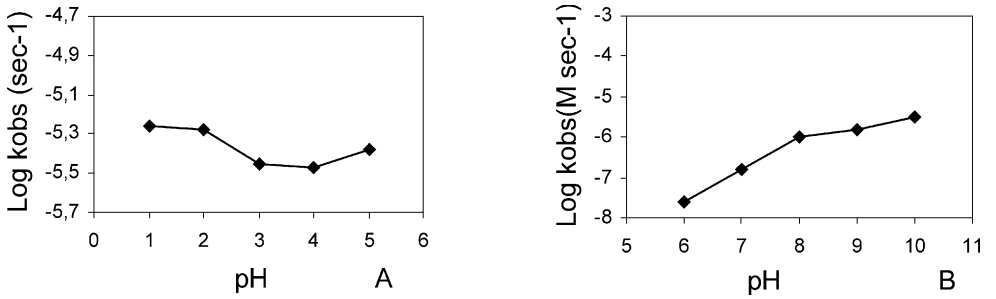

Fig. 6. (A) pH-Rate profile of NAMI-A at pH 1–5 ((pseudo) first-order kinetics); (B) pH-rate profile of NAMI-A at pH 6–10 (zero-order kinetics).

compared with degradation in 0.1 M phosphate and 0.1 M acetate at pH 9 and 3, respectively. No significant influence of the type of buffer at either pH was observed on the degradation rate of NAMI-A.

3.2.5. *Influence of temperature*

The influence of temperature on the degradation of NAMI-A was studied at pH 3 and 7 in the temperature range 4–37 °C. The Arrhenius relationship between the natural logarithm of k_{obs} and the reciprocal of the absolute temperature holds. The activation energy (E_a) at pH 3 was calculated to be 95.4 kJ/mol and its frequency factor (A) 3.60×10^{11} per s.

4. Conclusion

Degradation of NAMI-A follows (pseudo) first-order kinetics at pH values <6 and zero-order kinetics at pH values ≥ 6. No specific proton or hydroxyl catalysis was shown. The degradation rate and mechanism of NAMI-A are strongly pH-dependent. NAMI-A in solution is most stable in the pH region 3–4. Although an influence of buffer concentration was observed, no influence of specific buffer components could be determined. Temperature strongly influences the degradation rate of NAMI-A. These data, as well as those reported by Sava et al. (2002), imply that an acidic solvent should be used for NAMI-A administration during the clinical trials.

References

Bergamo, A., Gagliardi, R., Scarcia, V., Furlani, A., Alessio, E., Mestroni, G., Sava, G., 1999. In vitro cell cycle arrest, in vivo action of solid metastasizing tumors, and host toxicity of the antimetastatic drug NAMI-A and cisplatin. J. Pharmacol. Exp. Ther. 289, 559–564.

Bergamo, A., Zorzet, S., Gava, B., Sorc, A., Alessio, E., Iengo, E., Sava, G., 2000. Effects of NAMI-A and some related ruthenium complexes on cell viability after short exposure of tumor cells. Anti Cancer Drugs 11, 667–672.

Bouma, M., Nuijen, B., Jansen, M.T., Sava, G., Picotti, F., Flaibani, A., Bult, A., Beijnen, J.H., 2002. Development of a high-performance liquid chromatography method for pharmaceutical quality control of the antimetastatic ruthenium complex NAMI-A, J. Pharm. Biomed. Anal., in press.

Cocchietto, M., Sava, G., 2000. Blood concentration and toxicity of the antimetastatic agent NAMI-A following repeated intravenous treatment in mice. Pharmacol. Toxicol. 87, 193–197.

Martin, A.N. (Ed.), Physical Pharmacy (Chapter 12). Lea and Febiger, Philadelphia 1993.

Mestroni, G., Alessio, E., Sava, G., Pacor, S., Coluccia, M., Boccarelli, A., 1994. Water-soluble ruthenium (III)–dimethyl sulfoxide complexes: chemical behaviour and pharmaceutical properties. Metal Based Drugs 1, 41–63.

Sava, G., Cocchietto, M., 2000. Blood levels of ruthenium following repeated treatments with the antimetastatic compound NAMI-A in healthy beagle dogs. In Vivo 14, 741–744.

Sava, G., Capozzi, I., Clerici, V., Gagliardi, G., Alessio, E., Mestroni, G., 1998. Pharmacological control of lung metastases of solid tumours by a novel ruthenium complex. Clin. Exp. Metast. 16, 371–379.

Sava, G., Alessio, E., Bergamo, A., Mestroni, G., 1999. Sulfoxide ruthenium complexes: non-toxic tools for the selective treatment of solid tumour metastases. In: Clarke, M.J., Sadler, P.J. (Eds.), Biological Inorganic Chemistry, vol. 1. Springer, Berlin, Germany.

Sava, G., Clerici, K., Capozzi, I., Cocchietto, M., Gagliardi, R., Alessio, E., Mestroni, G., Perbellini, A., 1999. Reduction of lung metastasis by ImH[*trans*-$RuCl_4$(DMSO)Im]: mechanism of the selective action investigated on mouse tumors. Anti Cancer Drugs 10, 129–138.

Sava, G., Gagliardi, R., Bergamo, A., Alessio, E., Mestroni, G., 1999. Treatment of metastases of solid mouse tumours by NAMI-A: comparison with cisplatin, cyclophosphamide and dacarbazine. Anticancer Res. 19, 969–972.

Sava, G., Bergamo, A., Cocchietto, M., Flaibani, A., Gava, B., Pintus, G., Sorc, A., Tadolini, B., Ventura, C., Zorzet, S., 2000. Interaction of NAMI-A with the regulation of cell cycle progression. Clin. Cancer Res. 6, 4566s (abstract#501).

Sava, G., Bergamo, A., Zorzet, S., Sava, B., Casarsa, C., Cocchietto, V., Furlani, V., Scarcia, V., Serli, B., Iengo, E., Alessio, E., Mestroni, G., 2002. Influence of chemical stability on the activity of the antimetastasis ruthenium compound NAMI-A. Eur. J. Cancer 38, 427–435.

Vacca, A., Bruno, M., Boccarelli, A., Coluccia, M., Ribatti, D., Bergamo, A., Garbisa, S., Sartor, L., Sava, G., 2002. Inhibition of endothelial cell function and of angiogenesis by the metastasis inhibitor NAMI-A, Br. J. Cancer, 86, 993–998.

Zorzet, S., Bergamo, A., Cocchietto, M., Sorc, A., Gava, B., Alessio, E., Iengo, E., Sava, G., 2000. Lack of in vitro cytotoxicity, associated to increased G(2)–M cell fraction and inhibition of matrigel invasion, may predict in vivo-selective antimetastasis activity of ruthenium complexes. J. Pharmacol. Exp. Ther. 295, 927–933.